Towards a More Realistic Representation of Concrete Cracking for the Design of SHM Systems: Updating and Uncertainty Evaluation of Implicit Gradient Cracking Models

M. BREHM, T. J. MASSART and A. DERAEMAEKER

ABSTRACT

In the context of Structural Health Monitoring (SHM) systems, researchers are interested in generating virtual test data to design new or improve existing damage indicators. For some indicators based on local measurements, such as strains, the numerical models need to be able to represent the local behavior as accurately as possible.

In this paper, a numerical model of a notched concrete beam will be updated with respect to experimental load-deflection-curves using a CMA-ES (Evolution Strategy with Covariance Matrix Adaptation) optimization algorithm. Depending on the chosen objective function, several parameter sets of the constitutive law based on an implicit gradient cracking approach can be found, which lead to a suitable load-deflection-curve. For such optimized parameter sets, the resulting static strains are also similar for small damage levels, especially, when they are averaged.

1. INTRODUCTION

Structural health monitoring (SHM) systems are fully automated systems to be designed to replace expensive and time consuming maintenance works at structures and infrastructures. Hence, structural health monitoring systems are designed to monitor a structure and trigger an alarm, if a critical damage has occurred. Such systems consist typically of several sensors, a data acquisition unit, and a post processing unit.

Typically, damage is a local phenomenon, which can be visually recognized as a crack in a limited area of the structure, for instance. Therefore, sensor arrays or sensor networks measuring relative displacements or strains are frequently applied to detect

Maik Brehm, BATir - Structural and Material Computational Mechanics, Université Libre de Bruxelles, 50 av. F.D. Roosevelt, CP 194/2 1050 Bruxelles, Belgium, maik.brehm@ulb.ac.be

such local damage with high reliability. For example, [1] proposed the application of modal filters to extract a damage indicator based on sensor arrays using measured strains during vibrations. For the improvement of this indicator and its extension to the detection of cracks in concrete structures, virtual test data based on numerical models are inevitable to replace at least partly expensive full scale tests.

In the last three decades the interest in modeling local damage phenomena increased continuously, and therefore several damage models are available for various materials. Especially for concrete structures, continuum damage models should be preferred compared to discrete crack models, as during the initiation phase of concrete cracks the damage zone is larger than the discrete fully established crack. The non-local damage model developed in [2] and the equivalent implicit gradient damage model (e.g., [3]) are both appropriate for a realistic modeling of crack propagation in concrete.

A typical problem of complex damage models is the appropriate definition or identification of several model parameters. Some parameters are related to physical phenomena, other parameters are necessary to stabilize numerically the problem. For both types usually certain standard values are available from experience, but a high amount of uncertainty is still remaining. Most researchers, such as [4], prefer to fix the parameters to standard values, without investigating systematically the influence of their possible uncertainty. Only few researchers tried to tune the parameters to improve the coherence with experimental results.

A Markov estimation procedure was applied by [5] to update the gradient damage model according to [3] based on four-node bending and tensile tests of cellulose-fiber-reinforced cement mortar. Only three of eight uncertain parameters were used in the parameter tuning process to keep the numerical effort manageable. A similar study was performed by [6], where the squared Mahalanobis distance between numerical and experimental results was minimized by using a Kalman filter method. In contrast to [5] and [6], [7] used the non-local damage model of [2] to model the damage behavior of a notched beam subjected to a three-point-bending test. She used four out of eight possible uncertain parameters in the optimization process using a Leuvenberg-Marquadt algorithm.

In the present study, the implicit gradient damage model according to [3] is applied in combination with an exponential softening law. The parameters of the constitutive law are determined by using experimental data of a three-point-bending test of a notched concrete beam. The test and the respective results were provided in [8]. In contrast to the investigations by other researchers, all eight uncertain parameters are considered in the updating process. The objective function is a weighted Euclidean norm of 137 equidistant points at the load-deflection-curve until the total failure of the structure. The CMA-ES (Evolution Strategy with Covariance Matrix Adaptation) algorithm according to [9] is applied for the minimization of the objective function. It can be shown that the results of the identified parameters depend strongly on the weighting of the Euclidean norm used as objective function. Hence, several optimal parameter sets can be obtained that lead to similar load-deflection-curves.

Based on these optimal parameter sets, the local static strains along the longitudinal axis of the beam are calculated. The resulting averaged strains for small damages are almost identical. Hence, even though the parameters of the constitutive law cannot be uniquely identified, the model serves as a suitable numerical model to generate virtual strain test data, if one of the optimal parameter sets is applied.

2. DESCRIPTION OF DAMAGE AND CONSTITUTIVE LAW

The classical stress-strain relation of elasticity based damage mechanics at a certain point in the structure reads

$$\boldsymbol{\sigma} = (1 - D(\kappa))\boldsymbol{C}\boldsymbol{\varepsilon}, \tag{1}$$

whereas $\boldsymbol{\sigma}$ and $\boldsymbol{\varepsilon}$ are the stress and strain tensors and $\boldsymbol{C}$ the linear elastic material matrix. The damage function value $D(\kappa)$ is set to zero for undamaged materials and is otherwise a strictly increasing function of κ, which is the most critical strain experienced by the material. Whether a damage growth is finally possible or not is defined by the damage loading function

$$f(\bar{\varepsilon}, \kappa) = \bar{\varepsilon} - \kappa, \tag{2}$$

comparing a positive non-local equivalent strain measure $\bar{\varepsilon}$ to the most critical strain threshold variable κ. In addition, the Kuhn-Tucker relation needs to be fulfilled (e.g., [3]) for the damage loading function and the increase of κ.

Assuming an exponential softening law, the damage function is defined as follows

$$D(\kappa) = \begin{cases} 1 - \frac{\kappa_0}{\kappa}\left(1 - \alpha + \alpha \mathrm{e}^{-\beta(\kappa - \kappa_0)}\right) & : \kappa > \kappa_0 \\ 0 & : \kappa \leq \kappa_0 \end{cases}, \tag{4}$$

where κ_0 defines the initial linear elastic domain in terms of non-local equivalent strains.

As derived in [3], the non-local strain is given as the solution of the boundary value problem consisting of the Helmholtz equation

$$\bar{\varepsilon}(\boldsymbol{x}) - c\nabla^2\bar{\varepsilon}(\boldsymbol{x}) = \tilde{\varepsilon}(\boldsymbol{x}) \tag{5}$$

with appropriate boundary conditions. The calculation of the local equivalent strains $\tilde{\varepsilon}(\boldsymbol{x})$ at certain positions $\boldsymbol{x}$ of the structure is based on the modified von-Mises definition [10] to account for different sensitivities to tensile and compressive stress states.

3. DESCRIPTION OF EXPERIMENTS

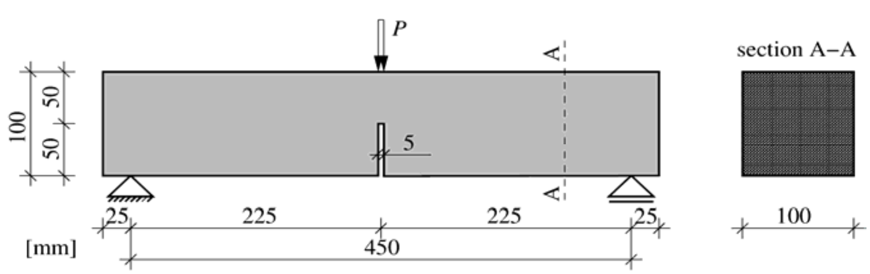

Figure 1. Geometry of test specimen according to [8].

The investigated concrete beam structure was tested by [8]. The system and the geometry of the three-point-bending test are described in Figure 1. The corresponding experimental load-deflection-curves are shown in Figure 2. The deflection is related to the vertical displacement at the center of the beam. Using all five experimental curves, a mean value curve and the corresponding standard deviation σ can be calculated for each coordinate of the load-deflection-curve. Based on information in [8] the most likely values and corresponding possible boundaries of the uncertain parameters can be identified, which are listed in Table 1.

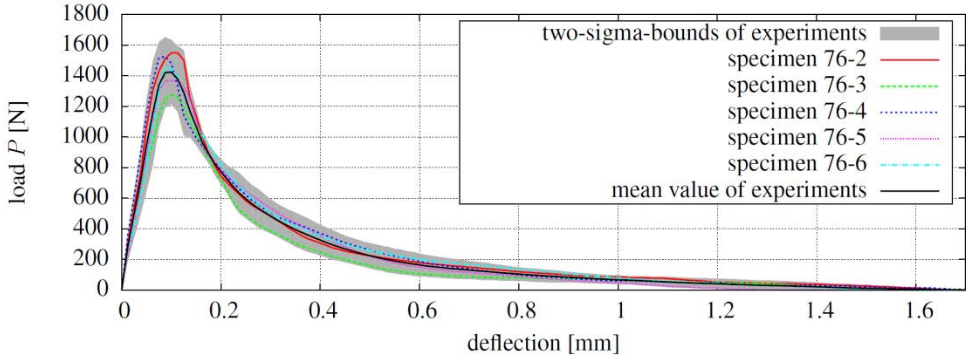

Figure 2. Results of single test specimens according to [8] and corresponding statistics.

Table 1. Initial parameter values and their boundaries for the damage model.

parameter	unit	initial	lower bound	upper bound
Young's modulus E	$\left[\frac{N}{m^2}\right]$	$1.84 \cdot 10^{10}$	$1.50 \cdot 10^{10}$	$2.30 \cdot 10^{10}$
Poisson ratio ν	$[-]$	0.2	0.1	0.3
compression strength f_c	$\left[\frac{N}{m^2}\right]$	$43.7 \cdot 10^6$	$38.3 \cdot 10^6$	$49.1 \cdot 10^6$
tension strength f_t	$\left[\frac{N}{m^2}\right]$	$2.61 \cdot 10^6$	$1.60 \cdot 10^6$	$4.20 \cdot 10^6$
α (acc. Eq.(4))	$[-]$	0.99	0.979	0.999
β (acc. Eq.(4))	$[-]$	175	70	200
density ϱ	$\left[\frac{kg}{m^3}\right]$	2300	2044.8	2484.2
$l_c = \sqrt{c}$ (acc. Eq.(5))	[mm]	1	0.5	1.5

4. INFLUENCE OF MESH COARSENESS AND DEAD LOAD

The damage model was implemented in a finite element code based on considerations of [3] assuming a plain stress behavior. A refinement strategy is applied, where triangular elements are used as transition elements between two scales of quadrilateral elements. The refinement of the mesh is conducted within an area of 5 by 7.5cm around the notch of the beam.

The load-deflection-curves of refined and non-refined meshes with different element sizes are contrasted with each other in Figure 3. All calculations are based on the initial parameter set according to Table 1. As the graphs of Figure 3 illustrate, the agreement between refined and non-refined meshes for equal lowest element sizes is almost perfect. Also the convergence to the true solution can be recognized. The coarse mesh with 5mm element size should be avoided. The element size refinement from 5mm to 2.5mm represents a good compromise between computation time and accuracy and is used for the following computations.

Another influencing factor is the dead load of the structure. The load-deflection-curves related to the initial parameter set according to Table 1 considering and neglecting the dead load for the calculations are presented in Figure 4. The differences related to the maximal load are approximately four per cent for the softening part of the load-deflection-curve. The influence of the dead load is not very strong. However, as the additional computational effort is manageable, the dead load is considered in all following calculations.

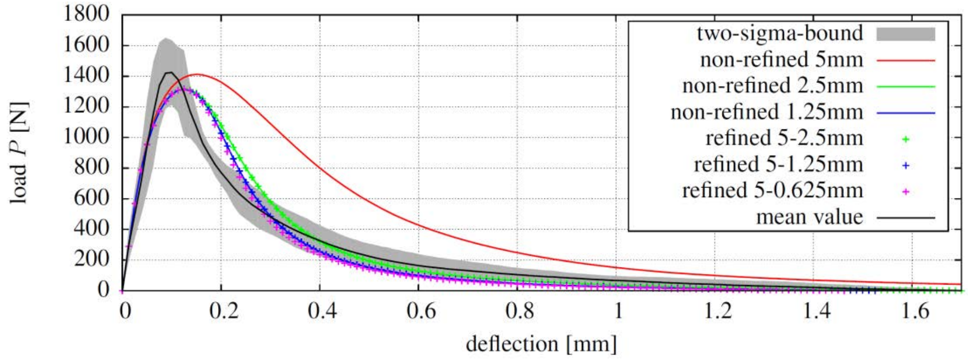

Figure 3. Comparison of load-deflection-curves of different meshes.

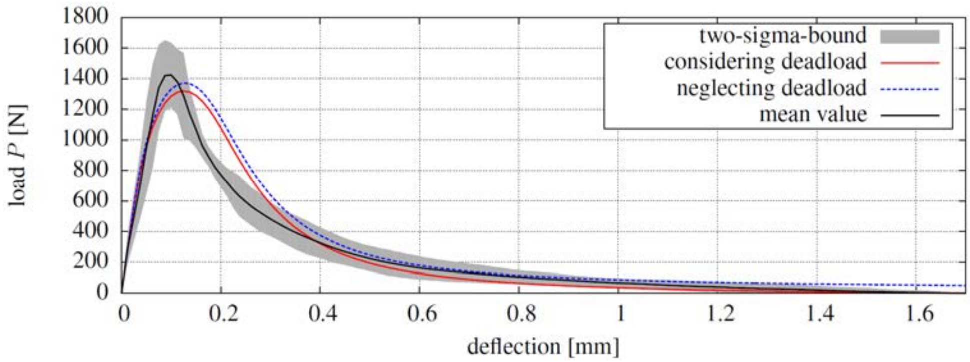

Figure 4. Comparison of load-deflection-curves considering and neglecting the dead load in the calculations.

5. MODEL UPDATING AND CORRESPONDING STATIC STRAINS

To identify the uncertain damage law parameters based on the test results of [8], any optimization strategy could be applied. Due to its user-friendliness and robustness, the CMA-ES (Evolution Strategy with Covariance Matrix Adaptation) algorithm according to [9] is applied in the present study. For all optimizations, the population size and the maximal number of function evaluations are set to 15 and 1500, respectively.

Nevertheless, it is important to define a suitable objective function. One possible measure is the weighted Euclidean distance

$$D(\boldsymbol{x}) = \sqrt{(\boldsymbol{z}_n(\boldsymbol{x}) - \mathbf{E}(\boldsymbol{z}_t))^{\mathrm{T}} \boldsymbol{W} (\boldsymbol{z}_n(\boldsymbol{x}) - \mathbf{E}(\boldsymbol{z}_t))}. \tag{6}$$

For the comparison, 137 equidistantly spaced points with respect to the deflection are defined at the load-deflection-curve. Therefore, the vectors $\mathbf{E}(\boldsymbol{z}_t) \in \mathbb{R}^{137}$ and $\boldsymbol{z}_n(\boldsymbol{x}) \in \mathbb{R}^{137}$ represent the mean value of the experimental load-deflection-curve and the numerical load-deflection-curve at the predefined points, respectively. The matrix $\boldsymbol{W} \in \mathbb{R}^{137\times137}$ is a weighting matrix. The vector $\boldsymbol{x}$ is related to one set of design parameters. Hence, the objective function

$$g(\boldsymbol{x}) = D(\boldsymbol{x}) \rightarrow \min \tag{7}$$

is defined by minimizing the weighted difference between the two load-deflection-curves.

Three different weighting matrices are investigated. The first weighting matrix $\boldsymbol{W_1} = \boldsymbol{I}$ is equal to the identity matrix, which leads to equally weighted residuals. The second weighting matrix $\boldsymbol{W_2} = \boldsymbol{C_t}^{-1}$ is the inverse of the full covariance matrix based on the statistics of the 137 equidistantly spaced points of the experimentally obtained load-deflection-curves. By using only the diagonal of the full covariance matrix $\boldsymbol{C_t}$, a third weighting matrix $\boldsymbol{W_3}$ is obtained.

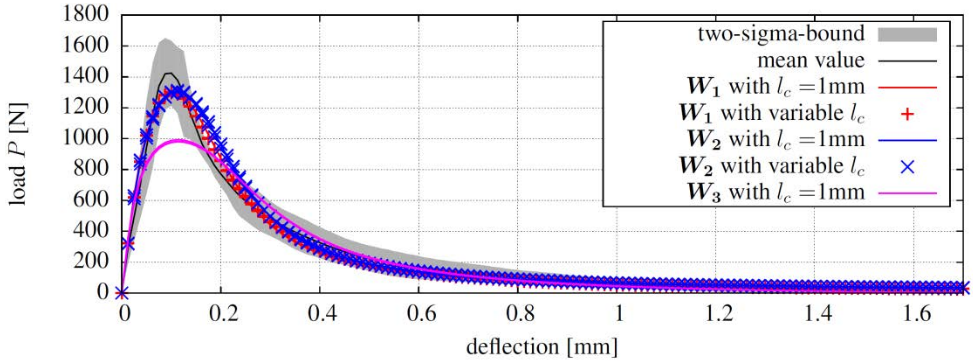

Figure 5. Load-deflection-curves for optimized parameter sets.

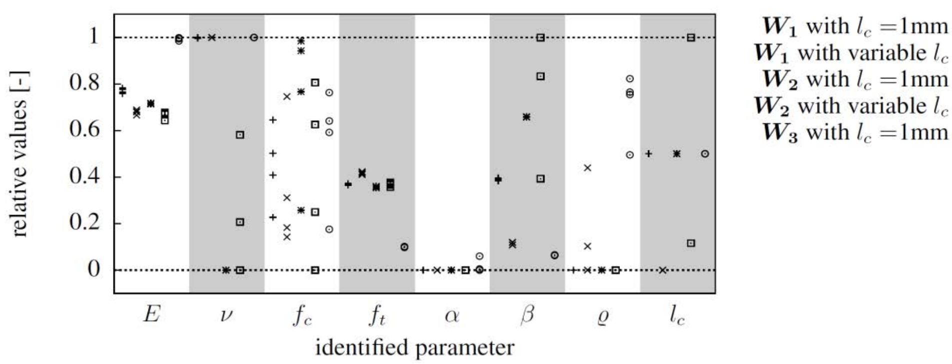

Figure 6. Optimized parameters in relation to their boundaries.

As the intrinsic length parameter l_c is the most critical parameter with respect to the energy dissipation and to mesh size dependent issues, the optimizations are performed by using a constant $l_c = 1\text{mm}$ and a variable l_c as described in Table 1. For each of the five optimization configurations, four independent optimization runs with identical settings are performed. The load-deflection-curves related to the optimal parameters of the constitutive law are shown in Figure 5. With the exception of using the weighting matrix $\boldsymbol{W_3}$, all results are very similar and acceptable.

Figure 6 depicts the identified parameters for each optimization configuration related to their boundaries. As the compression strength f_c and the mass density ϱ are insensitive parameters with respect to the objective function, an identification is almost impossible. In contrast, the Young's modulus E and the tensile strength f_t show a small variation with respect to the four different optimization runs and the different weighting matrices. The parameters β and l_c display a small variation regarding the four optimization runs. However, a large variation of these parameters is observed, if the different optimization configurations are compared. This indicates a certain coupling of these two parameters. The fact that no significant improvement can be obtained by including the parameter l_c into the set of design variables supports this assumption. Therefore, several different combinations of parameters can lead to very similar results for the load-deflection-curve.

As the static strains can be important for the design of SHM systems, they are extracted from the optimal system and compared with each other. Figure 7 illustrates the strains in longitudinal direction at a horizontal layer arranged 5mm on top of the notch tip. Of course, there are significant differences between the strains obtained with different optimization configurations especially at the position of the notch. In practice, it is very difficult to measure strains locally on the structure. Usually, the measured strains represent an averaged value with respect to a certain distance. Figure 8 shows such an averaging over 5cm at 9 points at the structure along the previously described layer. It can be observed, that the averaged strains are very similar especially for small damage levels.

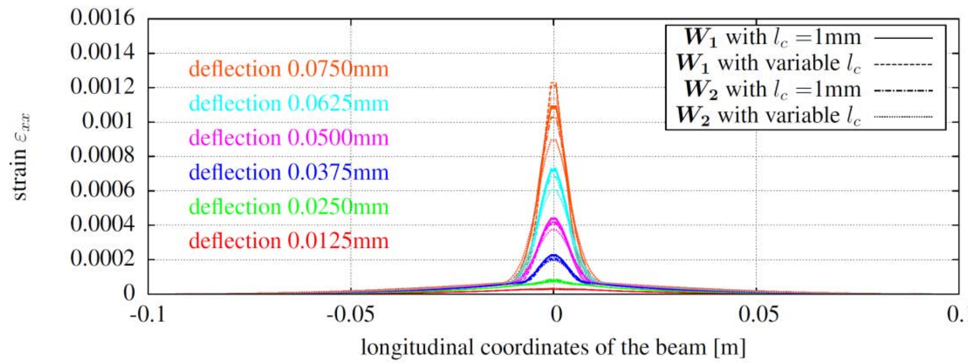

Figure 7. Strain distribution along the longitudinal axis of the beam at distance of 0.055m from the bottom of the beam.

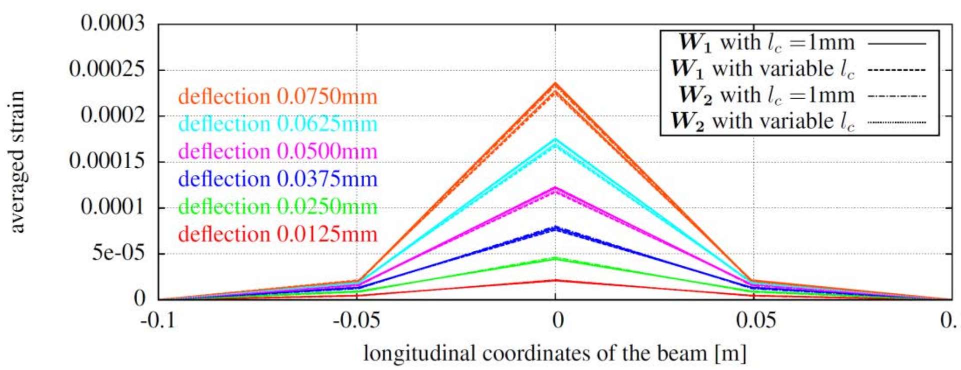

Figure 8. Averaged strain distribution along the longitudinal axis of the beam at distance of 0.055m from the bottom of the beam.

6. CONCLUSIONS AND DISCUSSIONS

This paper demonstrated for the case of a notched plain concrete beam that uncertain parameters of an implicit gradient damage model can be determined by means of experimental load-deflection-curves. However, not all parameters are uniquely identifiable. Some parameters are insensitive to the objective function and some parameters are coupled with each other, so that several valid solutions are possible.

A further investigation of the local static strains in longitudinal direction of the beam using the identified parameter sets revealed significant differences also for the strains near the damage. If the strains are averaged over a certain distance, as it is common in practice, the strains are very similar for small damage levels even for different parameter combinations of the damage law.

Consequently, as long as one of the optimized parameter sets is applied in the implicit gradient damage model, the numerical model provides a suitable basis to generate virtual test data, if the averaged static strains related to the longitudinal axis of the beam are the measure of interest.

REFERENCES

[1] A. Deraemaeker, K.Worden (Eds.), New trends in vibration based structural health monitoring, vol. 520 of CISM Courses and Lectures, chap. Vibration based structural health monitoring using large sensor arrays: Overview of instrumentation and feature extraction based on modal filters, SpringerWienNewYork, 19-54, 2010.

[2] G. Pijaudier-Cabot, Z. P. Bazant, Nonlocal damage theory, Journal of Engineering Mechanics 113:1512-1533, 1987 .

[3] R. H. J. Peerlings, Enhanced damage modeling for fracture and fatigue, Ph.D. thesis, Eindhoven University of Technology, Eindhoven, The Netherlands, 1999.

[4] J. G. Rots, Computational modelling of concrete fracture, Ph.D. thesis, Delft University of Technology, Delft, 1988.

[5] J. Carmeliet, Optimal estimation of gradient damage parameters from localization phenomena in quasi-brittle materials, Mechanics of Cohesive-frictional Materials 4:1-16, 1999.

[6] C. Iacono, L. Sluys, J. van Mier, Estimation of model parameters in nonlocal damage theories by inverse analysis techniques, Computer Methods in Applied Mechanics and Engineering 195(52):7211-7222, 2006.

[7] C. Le Bellégo, J. F. Dubé, G. Pijaudier-Cabot, B. Gérard, Calibration of nonlocal damage model from size effect tests, European Journal of Mechanics - A/Solids 22 (1):33-46, 2003.

[8] H. A. Körmeling, H. W. Reinhardt, Determination of the fracture energy of normal concrete and epoxy modified concrete, Report No. 5-83-18, Stevin Laboratory, Delft University of Technology, 1983.

[9] N. Hansen, S. Kern, Evaluating the CMA evolution strategy on multimodal test functions, in: Eighth International Conference on Parallel Problem Solving from Nature PPSN VIII, Springer, Berlin, 282-291, 2004.

[10] J. H. P. de Vree, W. A. M. Brekelmans, M. A. J.van Gils, Comparison of nonlocal approaches in continuum damage mechanics, Computers & Structures, 55(4):581-588, 1995.